03-14 March 2014

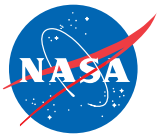

TECH BRIEFS

NATIONAL AERONAUTICS AND SPACE ADMINISTRATION

INTRODUCTION

Tech Briefs are short announcements of innovations originating from research and development activities of the National Aeronautics and Space Administration. They emphasize information considered likely to be transferable across industrial, regional, or disciplinary lines and are issued to encourage commercial application.

Additional Information on NASA Tech Briefs and TSPs

Additional information announced herein may be obtained from the NASA Technical Reports Server: **http://ntrs.nasa.gov**.

Please reference the control numbers appearing at the end of each Tech Brief. Information on NASA's Innovative Partnerships Program (IPP), its documents, and services is available on the World Wide Web at **http://www.ipp.nasa.gov**.

Technology Transfer Offices are located at NASA field centers to provide technology-transfer access to industrial users. Inquiries can be made by contacting NASA field centers listed below.

NASA Field Centers and Program Offices

Ames Research Center
Selected technological strengths: Information Technology; Biotechnology; Nanotechnology; Aerospace Operations Systems; Rotorcraft; Thermal Protection Systems.
David Morse
(650) 604-4724
david.r.morse@nasa.gov

Armstrong Flight Research Center
Selected technological strengths: Aerodynamics; Aeronautics Flight Testing; Aeropropulsion; Flight Systems; Thermal Testing; Integrated Systems Test and Validation.
Laura Fobel
(661) 276-3967
laura.j.fobel@nasa.gov

Glenn Research Center
Selected technological strengths: Aeropropulsion; Communications; Energy Technology; High-Temperature Materials Research.
Kimberly A. Dalgleish-Miller
(216) 433-8047
kimberly.a.dalgleish@nasa.gov

Goddard Space Flight Center
Selected technological strengths: Earth and Planetary Science Missions; LIDAR; Cryogenic Systems; Tracking; Telemetry; Remote Sensing; Command.
Nona Cheeks
(301) 286-5810
nona.k.cheeks@nasa.gov

Jet Propulsion Laboratory
Selected technological strengths: Near/Deep-Space Mission Engineering; Microspacecraft; Space Communications; Information Systems; Remote Sensing; Robotics.
Dan Broderick
(818) 354-1314
daniel.f.broderick@jpl.nasa.gov

Johnson Space Center
Selected technological strengths: Artificial Intelligence and Human Computer Interface; Life Sciences; Human Space Flight Operations; Avionics; Sensors; Communications.

John E. James
(281) 483-3809
john.e.james@nasa.gov

Kennedy Space Center
Selected technological strengths: Fluids and Fluid Systems; Materials Evaluation; Process Engineering; Command, Control, and Monitor Systems; Range Systems; Environmental Engineering and Management.
David R. Makufka
(321) 867-6227
david.r.makufka@nasa.gov

Langley Research Center
Selected technological strengths: Aerodynamics; Flight Systems; Materials; Structures; Sensors; Measurements; Information Sciences.
Kathy Dezern
(757) 864-5704
kathy.a.dezern@nasa.gov

Marshall Space Flight Center
Selected technological strengths: Materials; Manufacturing; Nondestructive Evaluation; Biotechnology; Space Propulsion; Controls and Dynamics; Structures; Microgravity Processing.
Terry L. Taylor
(256) 544-5916
terry.taylor@nasa.gov

Stennis Space Center
Selected technological strengths: Propulsion Systems; Test/Monitoring; Remote Sensing; Nonintrusive Instrumentation.
Ramona Travis
(228) 688-3832
ramona.e.travis@ssc.nasa.gov

NASA HEADQUARTERS

Daniel Lockney, Technology Transfer Program Executive
(202) 358-2037
daniel.p.lockney@nasa.gov

Small Business Innovation Research (SBIR) & Small Business Technology Transfer (STTR) Programs
Rich Leshner, Program Executive
(202) 358-4920
rleshner@nasa.gov

03-14 March 2014

TECH BRIEFS

NATIONAL AERONAUTICS AND SPACE ADMINISTRATION

Data Fusion for Global Estimation of Forest Characteristics From Sparse Lidar Data

A new approach automatically produces a hierarchical set of image segmentations for detailed analysis of forest data.

Goddard Space Flight Center, Greenbelt, Maryland

This lidar data fusion approach is based on associating samples from sparse lidar data with groups of region objects determined by a unique image segmentation approach, HSeg (Hierarchical Segmentation). This segmentation approach, which was previously developed by co-innovator James Tilton, is ideal for this application because HSeg automatically produces a hierarchical set of image segmentations, i.e., a set of several image segmentations of the same image at different levels of detail in which the segmentations at coarser levels of detail can be produced from simple merges of regions at finer levels of detail. This enables a simple approach for selecting an appropriate level of segmentation detail. HSeg also automatically classifies the spatially continuous region objects into region classes, through a tight intertwining of region growing segmentation, which produces spatially connected region objects, with non-adjacent region object aggregation, which groups sets of region objects together into region classes. No other practical, operational image segmentation approach has this tight integration of region growing, object finding with non-adjacent region aggregation. HSeg produces image segmentations with high spatial fidelity — enabled by the tight intertwining of region growing segmentation with non-adjacent region object aggregation.

Also, Hseg controls the importance of spatially adjacent region merging relative to spatially non-adjacent region merging (aggregation) through the S_{wght} parameter, which can vary from 0.0 to 1.0. At S_{wght} = 0.0 no non-adjacent region object aggregation is performed, and with S_{wght} = 1.0, equal weighting is given to spatially adjacent and spatially non-adjacent region merging.

The initial tests were performed using Landsat TM data transformed into brightness, greenness, and wetness tasseled cap features in an area where there is "wall-to-wall" lidar data from the Laser Vegetation Imaging Sensor, LVIS. This Landsat TM data was collected on Sept. 5, 2007 from over central Maine, and the LVIS data was collected in August 2009. The spaceborne lidar (SSL) data was simulated by selecting tracks out of the LVIS data at an appropriate density. The LVIS data served as the ground reference data for the evaluation of the results.

Later, additional tests were performed using UAV SAR data with three polarizations: HH, HV, and VV. The original SAR data was at 5-meter pixel resolution, but 6×6 blocks of pixels were averaged of this data to produce 30-meter pixel resolution SAR data to better compare the results with the tests with the 30-meter transformed Landsat TM data.

This work was done by James Tilton, Bruce Cook, and Paul Montesano for Goddard Space Flight Center. Further information is contained in a TSP (see page 1).GSC-16535-1

Debris & Ice Mapping Analysis Tool — Database

The software is simple for engineers and management to use.

Lyndon B. Johnson Space Center, Houston, Texas

The Debris & ICE Mapping Analysis Tool (DIMAT) system is a Web-based system that supports communication, data integration, data sharing, and problem definition/resolution through use of an integrated presentation framework for ice and debris description and analysis. It provides an integrated engineering problem description, visualization analysis, and resolution presentation framework for ice and debris issues. These include, but are not limited to: pre-launch debris walk-downs; ice formation during tanking, pre-launch, and launch; debris hits on Orbiter identified on-orbit or post-landing; and external tank (ET) foam damage/texture mapping. The DIMAT system leverages the EMaps application and models, as well as Design Visualization Group (DVG) models to provide high-fidelity 3D models of the Orbiter, ET, Solid Rocket Boosters (SRB), and Pad. Proposed solutions generated by DIMAT integrate these models with ice/frost/debris location data, and can include 3D visualizations and digital photographs of ice and/or orbiter TPS (thermal protection system) debris hits. Ice/debris displayed on the EMaps model will represent actual size and location. The user will be able to access data and photograph displays by selecting the ice on the EMaps model.

The DIMAT analysis component allows the user to enter ice/debris data into the system from the Web, and to link to program-related databases and documents. The DIMAT inspector component is a laptop-based system that the ice/debris team uses to enter data, including digital photographs, in real time. It incorporates the diverse data repositories into a single database.

The software is simple for engineers and management to use, and automates data input into a repetitive report. The software easily adapts to another database

and is comparative to system architecture. The model will be capable of being utilized for engineering analysis, and integrates and displays CAD-based drawings. The model can display integrated views/JPEGS from NSTS documents.

DIMAT can display and translate between any of the element coordinate systems, and has the ability to calculate *x,y,z* from manual/visual user input. Using *x,y,z* coordinates provides relative distances or clearances between points. It visually locates ice/debris on the model and determines *x,y,z* location. It has the ability to provide accurate size/geometry of reported ice/debris, and can isolate specific zones for identifying locations of ice/debris and surrounding hardware.

The model will contain locations, type, field of view, and simulated camera view for specified OTVs (Orbital Transfer Vehicles), and has the capability to link OTV to the application to display real-time status/picture of reported ice/debris. The model will have the capability to accept live feed from a selected OTV and overlay on the model.

This work was done by Robert Luecking and Cindy Nguyen of The Boeing Company for Johnson Space Center. Further information is contained in a TSP (see page 1). MSC-25030-1

Data Acquisition and Processing Software — DAPS

Langley Research Center, Hampton, Virginia

DAPS was designed to support the DAWN-AIR project participating in the Genesis and Rapid Intensification Processes (GRIP) hurricane campaign. It controls the data acquisition system consisting of a scanner that directs the lidar beam, an inertial navigation system/GPS (INS/GPS) unit for monitoring aircraft motion, a DSP module, and serial and video modules while acquiring and processing lidar data in real time. DAPS was optimized to meet the project requirement: acquiring and processing more than 550,000 samples per second. DAPS was capable of managing such extensive computational loads without experiencing a single incident of crash or system failure during the entire 130 flight hours of the GRIP mission.

The latest wind profiling algorithm accurately estimates the horizontal wind speed and direction. It is robust enough to identify abrupt changes in the horizontal wind parameters that are difficult to be detected by other conventional methods. Some of the unique features of DAPS and the latest data processing algorithm are as follows:

1. DAPS can operate both in real time and offline while performing full tasks faster than 10 Hz of execution rate.
2. DAPS has informative data displays such as the Doppler shift and the power distribution of line of sights, horizontal and vertical wind profiles, and color-coded history displays of wind profiles. It also displays important user inputs and real-time GPS data.
3. DAPS is smart software that is capable of automatic error correction and calibration of the scanner and the digitizer.
4. DAPS is robust and is capable of long-haul operations without an incident of system error or crash.
5. The latest wind profiling algorithm can produce robust horizontal wind parameters.
6. The algorithm has smart routines to increase the signal-to-noise ratio and effective INS/GPS data interpretation and application.
7. The algorithm runs at the minimal error resolution of 1 m/s in wind speed with 512-FFT.

This work was done by Jeffrey Beyon of Langley Research Center. Further information is contained in a TSP (see page 1). LAR-18033-1

Metal-Assisted Fabrication of Biodegradable Porous Silicon Nanostructures

Silicon nanostructures are fabricated from single-crystal silicon by an electroless chemical etch process.

Lyndon B. Johnson Space Center, Houston, Texas

Porous silicon nanowires are fabricated by two-step, metal-assisted electroless chemical etching of p-type or n-type silicon wafers. This method, in combination with nanolithography or nanopatterning, can be applied to fabricate porous silicon nanostructures of different shapes and sizes, such as nanorods, nanobelts, nanostrips, and nanochains. The specific resistivity of the silicon substrate, and composition of the etching solution, determine the porosity and pore size or lack thereof of the resulting nanostructures. Silicon doping, type of metal catalyst, concentrations of H_2O_2, and solvent all affect the formation of porous nanostructures at various resistivity ranges of silicon. A phase diagram summarizing the relation of porosification and doping, metal, concentrations of H_2O_2, and solvent can be generated.

In this innovation, high-aspect-ratio porous silicon nanostructures, such as those previously mentioned, were fabricated from single-crystal silicon by an electroless chemical etch process. A metal film, metal nanofeatures, or metal nanoparticles were coated on the silicon substrate first, and a solution of HF and hydrogen peroxide was then used to anisotropically etch the silicon to form the porous silicon nanostructures. Up to hundreds of micron-long high-aspect-ratio porous silicon nanostructures can be fabricated, and the patterns of the cross-section of porous silicon structures can be controlled by photolithography, nanolithography, or nanoparticle-assisted patterning. The porosity is related to the resistivity range of the silicon substrate, the metal catalysts, the chemical concentration, and the additive solvent. The fabricated porous silicon nanostructure is biodegradable, and the degradation time can be controlled by surface treatments.

Porous silicon nanowires can be fabricated with a two-step process. A nanostructured metal layer can be deposited on a silicon substrate by an electroless chemical deposition or electrochemical deposition. This step determines the shape of the final nanowires. Alternatively, metal nanoparticles can be spun on the silicon surface to form a metal layer, or a metal layer can be physically or chemically deposited on the silicon through a nanopatterned mask. The metal-coated silicon can be etched in a solution of HF, water, and H_2O_2 to produce porous silicon nanowires. Solvent can be added to the solution to modulate the features of the porous silicon nanowires.

This work was done by Mauro Ferrari, Xuewu Liu, and Ciro Chappini of the University of Texas Health Science Center at Houston for Johnson Space Center. For further information, contact the JSC Innovation Partnerships Office at (281) 483-3809.

In accordance with Public Law 96-517, the contractor has elected to retain title to this invention. Inquiries concerning rights for its commercial use should be addressed to:

The University of Texas
Health and Science Center at Houston
Office of Technology Management
7000 Fannin Street, Suite 720
Houston, TX 77030

Refer to MSC-24690-1, volume and number of this NASA Tech Briefs *issue, and the page number.*

Post-Growth, *In Situ* Adhesion of Carbon Nanotubes to a Substrate for Robust CNT Cathodes

This technology can be used down-hole in oil wells, and in high-temperature, high-pressure, corrosive environments in the automotive industry.

NASA's Jet Propulsion Laboratory, Pasadena, California

The field emission electron sources using carbon nanotubes (CNTs) are being targeted for low-power vacuum microelectronic applications for harsh-environment operation (high temperature, pressure, and corrosive atmosphere). While CNTs have demonstrated excellent properties in terms of low threshold field, low-power operation, and high current densities, one problem with vacuum electronic applications is poor adhesion of CNTs to the substrate on which they are synthesized. The chemical vapor deposition (CVD) process used to grow CNTs on silicon or other metallic substrates using an iron catalyst with a thin oxide diffusion barrier layer has consistently provided reproducible growth. The CNTs are only surface-adhering in these cases, and are easily removed from the surface with the application of minor forces — typically pressures of 20 to 60 kPa. This causes catastrophic failures of CNT field emitters since the applied field could exceed the adhesion strength of CNTs to the substrate.

An *in situ* process was developed that allows welding of CNT bundles to the support substrate. An efficient field emission architecture of CNTs has been

reported and patented by JPL. This architecture consists of arrays of CNT bundles of 1 to 2 micrometers in diameter, spaced 5 micrometers apart. These bundles can be grown on any substrate that is conducive for lithographic patterning and catalyst deposition for CNT growth (Fe, Ni, etc.). A diffusion barrier layer, typically an oxide layer, is deposited underneath the metal catalyst.

Growth of CNTs on titanium substrate with a diffusion barrier at 575 to 600 °C has been demonstrated. Following the growth process, the CNT bundle arrays are welded into Ti by heating the Ti substrates to 1,050 °C such that the surface of Ti softens and the CNTs get rooted inside. This welding process provides CNT field emission samples that are robust and are tightly bound to the substrate. They have been shown to withstand high electric fields without getting dislodged.

The novelty here is the single process step that allows the growth and *in situ* welding to produce vertically aligned, patterned CNTs on a metallic substrate. Even though the process was developed for titanium substrate, it is possible to implement the same with other metallic substrates and catalyst combinations. It is possible to deposit any of the metal layers on any other metal substrates to create a multi-metal substrate on which CNT bundle arrays or simply CNTs are grown. The main advantage is that it allows creation of array patterns of CNTs, and welds them into place as opposed to previously reported processes that required depositing loose CNTs on metallic films followed by a welding process. It is not possible to achieve vertically oriented and patterned CNTs with such a welding process.

This work was done by Harish Manohara, Valerie Kristof, and Risaku Toda of Caltech for NASA's Jet Propulsion Laboratory. Further information is contained in a TSP (see page 1).

In accordance with Public Law 96-517, the contractor has elected to retain title to this invention. Inquiries concerning rights for its commercial use should be addressed to:

Innovative Technology Assets Management
JPL
Mail Stop 321-123
4800 Oak Grove Drive
Pasadena, CA 91109-8099
E-mail: iaoffice@jpl.nasa.gov

Refer to NPO-48953, volume and number of this NASA Tech Briefs *issue, and the page number.*

Integrated PEMFC Flow Field Design for Gravity-Independent Passive Water Removal

The design solves safety as well as reliability issues.

Lyndon B. Johnson Space Center, Houston, Texas

A gravity-independent PEM (proton exchange membrane) fuel cell stack has been developed that will operate at high-pressure H_2 and O_2 conditions with the requirement for relatively modest H_2 and O_2 gas circulation. Until now, in order to get higher efficiency, excess reactant gas flow was required to prevent water slug formation in gas channels, thus reducing fuel cell performance. In addition, this excess gas flow is typically supported by mechanical pumps and/or a high-pressure ejector system. All of these in a closed space environment contributed to potential safety as well as reliability issues due to the potential failure of mechanical pumps and ejectors.

ElectroChem's Integrated Flow Field (IFF) design for a PEM fuel cell solves all these issues. It is based on a multilayered integrated flow-field structure that forms a porous structure with distinct wetting properties. It results in increased exposure of the catalyst to the reactant gas, resulting in higher cell voltage. This results in higher efficiency than the conventional plate designs. In addition, the entire flow field makes full contact between the porous structure and the electrodes, thus avoiding damage to membrane electrode assemblies (MEAs) at elevated operating pressure conditions. The same design also provides transport of product water back to the entire flow field for humidification and greater performance.

In the IFF cell there is no need for excess reactant gas, since the design is based on a non-flow-through operation. The IFF fuel cell allows the operation at 100% reactant gas utilization. The design also enables passive removal of water at various cell orientations.

The figure demonstrates a complete passive water removal at non-flow-through operation condition and a response to

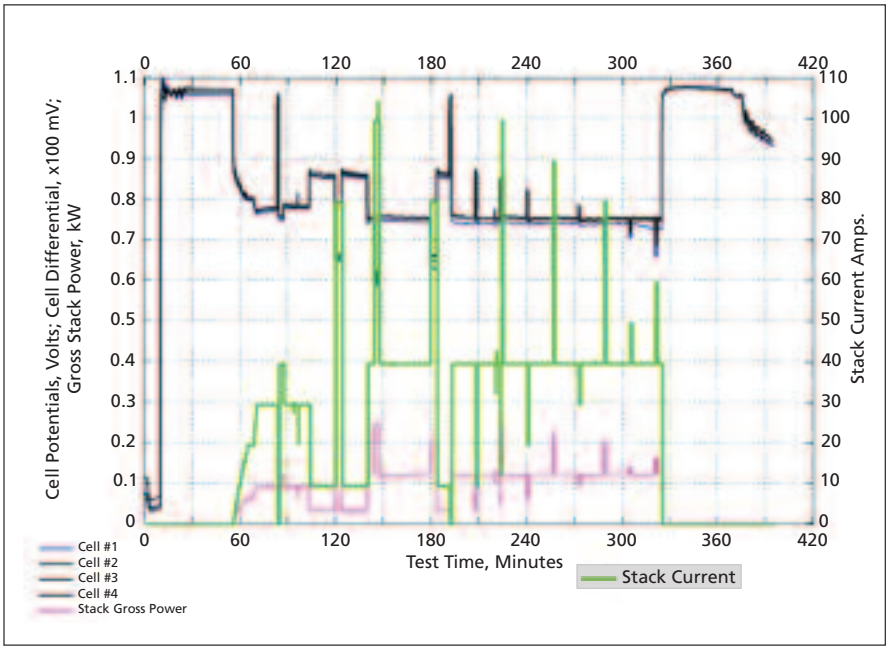

Demonstration of a **Non-Flow-Through Fuel Cell Operation** following NASA load profile testing. The IFF fuel cell performed passive water removal without gas circulation.

3–1 power ratio demand. It is an IFF fuel cell stack with 4 cells of 200 cm^2 electrode surface area.

The results of IFF fuel cell configuration have demonstrated 100% reactant gas utilization, reduced cost and weight penalties, and system simplification with higher reliability.

This IFF design was developed for use in a PEM fuel cell power plant for space application, but it could also be used for high-altitude balloon flight and air-independent applications (e.g., manned and unmanned underwater vehicles). When the IFF design is used in a PEM electrolyzer, it functions as an internal phase separator, which enhances overall system efficiency.

This work was done by Michael Pien of ElectroChem, Inc. for Johnson Space Center. Further information is contained in a TSP (see page 1).

In accordance with Public Law 96-517, the contractor has elected to retain title to this invention. Inquiries concerning rights for its commercial use should be addressed to:

Michael S. Pien, Ph.D.
Vice-President of Research and Development
ElectroChem, Inc.
400 W Cummings Park # 5600
Woburn, MA 01801
Phone No.: (781) 938-5300
E-mail: sales@fuelcell.com

Refer to MSC-24587-1, volume and number of this NASA Tech Briefs *issue, and the page number.*

Thermal Mechanical Preparation of Glass Spheres

The forming process allows a very wide variety of material to be processed into spheres.

Marshall Space Flight Center, Alabama

Samples of lunar regolith have included small glass spheres. Most literature has suggested the small spheres were formed by meteorite impacts. The resulting transformation of kinetic energy to thermal energy caused the lunar surface to melt. The process yielded glass spheres. Recreating a meteorite impact that yields glass spheres is very challenging. Furthermore, the melting temperature of certain minerals on the Moon precludes the use of standard thermal techniques.

Glass spheres are created by using a thermal and pneumatic process. The process allows extremely high-melting-temperature material to be transformed into sub-750-micron spheres. The thermal and mechanical process developed transforms the molten material to the lowest energy morphology, a sphere, while locking in the glass chemistry.

To produce a high volume of sub-750-micron glass spheres, the feedstock material was melted with a plasma system. The system uses high-power, remotely coupled electric plasma. The molten material is then routed through a molybdenum orifice and allowed to fall vertically by gravity. Approximately one meter from the discharge, a high-velocity pneumatic jet is positioned perpendicular to the glass stream. At the impingement zone, the molten glass material is pneumatically removed from the primary stream path and rapidly cooled to glass morphology while traveling to the collection area. At the collection area, the spheres are mechanically collected.

The integrated plasma system and mechanical forming process allow a very wide variety of material to be processed into spheres. Also, the rapid pneumatic quench locks ensure glass morphology and precludes any significant devitrification.

Glass spheres are currently used in a wide variety of consumer and commercial applications. The ability to thermally react feedstock materials at plasma temperatures extends the range of possible glass chemistries available. The demonstrated ability to produce spheres directly from a molten glass stream increases the upper diameter limit realized in traditional solid to sphere processes. Examples of current research work using the plasma process include production of high-strength glass spheres for drilling proppants, and the integration of catalyst materials in bio-degradable glass for ground water remediation applications.

This work was done by Mike Weinstein of Zybek Advanced Productions, Inc. for Marshall Space Flight Center. For more information, contact Sammy Nabors, MSFC Commercialization Assistance Lead, at sammy.a.nabors@nasa.gov. Refer to MFS-32938-1.

Mechanistic-Based Multiaxial-Stochastic-Strength Model for Transversely-Isotropic Brittle Materials

The methodology is applicable to a wide variety of graphite, coatings, and composite materials.

John H. Glenn Research Center, Cleveland, Ohio

A methodology has been developed and the software written to predict the probability of failure of transversely isotropic (a type of anisotropy) materials under generalized thermomechanical loading. This methodology is mechanistic in that it is based on the physical characteristics of brittle fracture, and morphological in that it considers the size, shape, and orientation distribution of strength controlling defects or flaws. On that basis, it can also account for a material's failure modes and direction of damage initiation from loading. It is capable of predicting an anisotropic material's probability of failure under transient and cyclic loading. This innovation can be applied to materials such as graphite, coatings, or the individual brittle constituents of composite materials.

The strength of an isotropic brittle material is independent of the direction of the applied load. However, for many brittle materials, the strength of the material changes with the direction of the applied load. These are termed anisotropic materials. The most common type of material strength anisotropy is transverse isotropy, where material strength is isotropic within a plane but orthogonal to that plane, the strength is greater than or less than the in-plane strength.

The unit sphere methodology is an attempt to provide an improved mechanistic basis to the problem of predicting strength response of an anisotropic and composite material under multiaxial loading as compared to polynomial interaction equation formulations. It has multiple unique features including flaw orientation and fracture toughness anisotropy. These physically based anisotropy functions are general and can model tightly defined or more diffuse material anisotropy textures describing flaw populations. Innovative equations were developed in order to achieve this capability. The methodology also includes consideration of strength scatter to predict material probability of failure, shear sensitivity of flaws, and accounting for multiple failure modes regarding overall failure response. One novel feature of this methodology is the ability to predict the orientation of critical flaws under multiaxial loading.

With this capability, the model can be tuned to the physical attributes of the material by, for example, mapping the toughness response of the material with respect to orientation for indentation testing, or mapping the observed orientation anisotropy of the pre-existing flaws in the material. In principle, by this methodology, the physical attributes of the anisotropic material can also be used to predict the multiaxial strength response of the material.

It is intended for aerospace applications where trade-offs must be performed regarding safety, durability, and weight. It is anticipated that this software will be used with finite element or micromechanics-based codes describing the behavior of composite materials. This incorporation would allow the full exercise of the new methodology, including incremental time/load steps, and fatigue of composite laminates and woven composite structures.

This work was done by Noel N. Nemeth of Glenn Research Center. Further information is contained in a TSP (see page 1).

Inquiries concerning rights for the commercial use of this invention should be addressed to NASA Glenn Research Center, Innovative Partnerships Office, Attn: Steven Fedor, Mail Stop 4–8, 21000 Brookpark Road, Cleveland, Ohio 44135. Refer to LEW-19018-1.

Methods for Mitigating Space Radiation Effects, Fault Detection and Correction, and Processing Sensor Data

A combination of three innovations enables increased efficiency, stability, and flexibility of data management and systems functionality.

Lyndon B. Johnson Space Center, Houston, Texas

The Integrated Modular Avionics (IMA) architecture being developed for space applications requires that sensor data be autonomously sampled and transmitted to the system network. This transmission needs to occur on a predetermined, fixed schedule to avoid conflicts on the network. It needs to be capable of building packets of sensor data for individual application partitions (i.e., environmental control, propulsion, and vehicle management). It must be easily configured for flexibility in system scheduling.

Once a minor frame interrupt (MFI) is received from the network, the timing within a frame begins. The poll list table controls the timing. It starts the input/output module (IOM) sample list execution within each IOM. After enough time has elapsed for the IOMs to step through their respective sample lists, the poll list initiates the command to start assembling the packets. These may include, for example, a packet that contains only data for the environmental control system, another packet could include data for the propulsion system, and yet another packet may contain RIU (remote interface unit) status information. These packets are transferred to the network interface card (NIC). The tables in the NIC schedule the transmission onto the network for each packet. The tables may be unique by minor frame. This allows different packets of data to be sent on different minor frames of the system schedule.

Self-checking lockstep processor architectures, by their nature, are intended to detect differences between redundant elements and to prevent their further propagation. Traditional methods of dealing with detected differences between the halves of a lockstep processor pair are to cease lockstep operation and to initiate recovery. In an integrated processor application, ceasing lockstep operation impacts all software applications on the platform, as they are unable to perform their function until the recovery has been completed and lockstep operation is resumed. The method being described here eliminates the loss of lockstep operation under certain conditions such that the recovery can be done "seamlessly" to all applications other than the one directly accessing the resource that caused the detected difference between lockstep halves.

The Orion VMC (vehicle management computer) processor design is based upon the re-use of a processor design from a commercial avionics product. That design includes the use of several commercial off-the-shelf (COTS) components for which there are no equivalent space-rated components. One of those COTS components is NOR flash that is used to store program and database information for the processor. A design solution that maximizes the advantages of re-use, while satisfying the radiation requirements of the product when using these COTS NOR flash devices in the program flash array, was needed.

This work was done by Mike Bartels, Dean Sunderland, Terry Ahrendt, Tim Moore, David Yeager, Kevin Stover, James Tyrrell, and Bob Poucher of Honeywell for Johnson Space Center. Further information is contained in a TSP (see page 1).MSC-24769-1/81-1/5-1.

Compact Ka-Band Antenna Feed with Double Circularly Polarized Capability

This design could be used for the feed component in high-gain antennas.

Goddard Space Flight Center, Greenbelt, Maryland

NASA has an interest in utilizing the Ka-band frequency allocation. One of the main reasons for migrating to Ka-band is the need for higher frequency bandwidth to enable higher data rates. A dual circular polarized wideband antenna for Ka-band communications applications was designed leveraging a novel Ka-band polarizer design used in Lunar Reconnaissance Orbiter/Solar Dynamics Observatory (LRO/SDO). The proposed design merges two components (polarizer and antenna) into one unit, reducing its overall size. Its simulated bandwidth extends beyond the allocated bandwidth for NASA at Ka-band. This novel design could be used as well for the feed component in high-gain antennas (HGAs).

Satellite communications at the Ka-band frequencies has been a topic of interest for the last decade. NASA has had a Ka-band frequency allocation underused for many years due to various reasons. When the transmitter's output data rate after encoding is 450 Msps, the spectrum needs to be severely filtered to avoid interference with NASA's DSN frequency allocation, which promotes large amounts of intersymbol interference at the receiver. Transitioning to Ka-band will mitigate this problem since the allocated band-

width is larger, allowing much higher data rates to be sustained without such signal distortions.

The Earth-shaped reflector antenna at Ka-band consists of a single reflector configuration where the feed is located at the focal point of the system using supporting struts, and the reflector is shaped to produce an Earth-shaped radiation pattern. The waveguide used to carry energy to the antenna feed can be located along one of, or be part of, the struts supporting the feed above the reflector.

The antenna design consists of merging a corrugated feed antenna with a polarizer to produce a satisfactory solution of blockage reduction (size reduction) of the reflector aperture. What is usually a two-component system has been reduced to a single part, reducing mass, size, and cost. This antenna could be used in Ka-band HGA or Earth-shaped antenna reflector combinations. The polarizer/antenna combination also allows it to be used in dual circular polarization applications. The overall return loss is better than 20 dB for the simulated frequency range of 23.5 to 28.5 GHz, showing an excellent impedance match over NASA's frequency allocation. The port isolation between the ports has not been optimized, but can be optimized for the application at hand.

For the current design, the isolation for the standalone feed antenna and polarizer combination varies between –15 to –18 dB over the frequency band. For a standalone application (no reflector), this could be improved by improving the internal wave impedance match between the polarizer and feed antenna. For a reflector application, it can be optimized to partially cancel the reflection from the reflector back into the feed, which is typically of the same order of magnitude.

This work was done by Cornelis du Toit of QSS and Kenneth Hersey of MEI Technologies for Goddard Space Flight Center. Further information is contained in a TSP (see page 1). GSC-16773-1

Dual-Leadframe Transient Liquid Phase Bonded Power Semiconductor Module Assembly and Bonding Process

This module package and bonding process enable device operation at temperatures exceeding 400 °C.

John H. Glenn Research Center, Cleveland, Ohio

A high-temperature-capable wide-bandgap semiconductor power module package, coupled with a new high-temperature-capable bonding process (with an optimized assembly and manufacturing process), has been developed that, together, can allow device operation at temperatures exceeding 400 °C, with the potential for higher-temperature operation depending on the semiconductor device characteristics.

The semiconductor module is an ultra-compact, hybrid power module that uses double leadframes and direct leadframe-to-chip transient liquid phase (TLP) bonding. The unique advantages include very high current-carrying capability, low package parasitic impedance, low thermomechanical stress at high temperatures, double-side cooling, and modularity for easy system-level integration. The new power module will have a very small form factor with 3 to 5× reduction in size and weight from the prior art, no failure-prone bond wires, and will be capable of operating from 450 to –125 °C.

Traditional power semiconductor modules use solder to attach the die to the substrate, which requires that the device be heated to a temperature higher than the normal operating temperature. For very-high-temperature-operation devices, it isn't feasible to use a soldering process. However, in this innovation, the

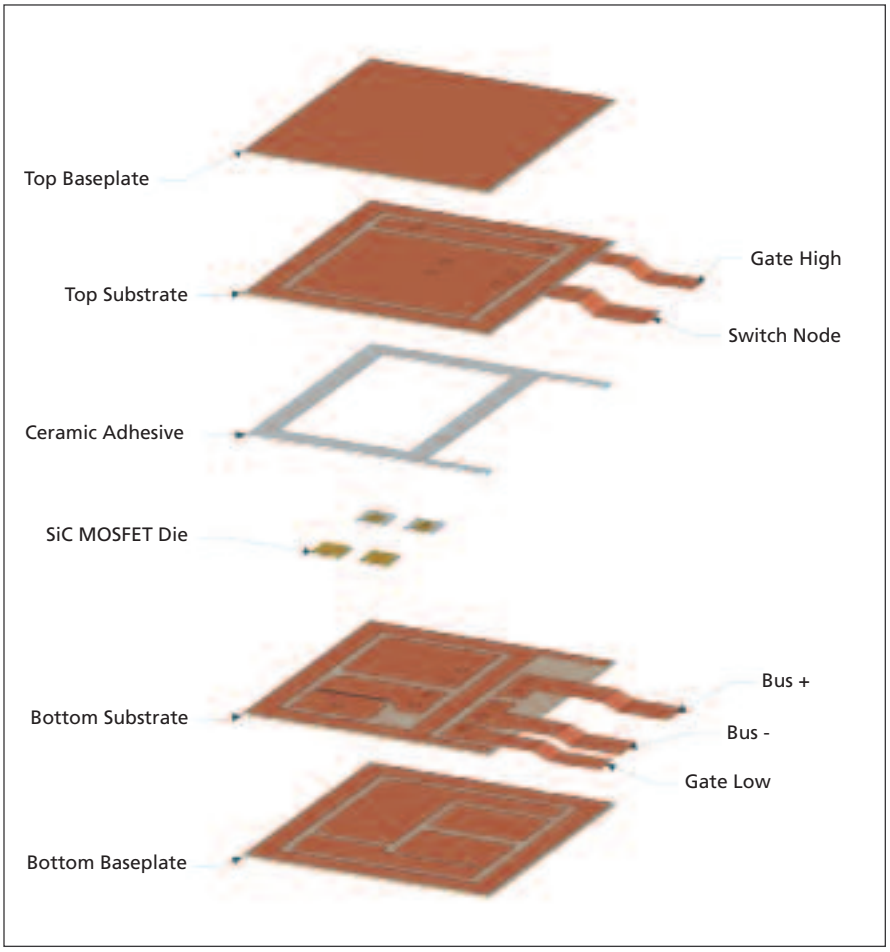

An exploded view of the **Semiconductor Module** stackup.

Transient Liquid Phase (TLP) bonds at a temperature between the operations temperature range of the device. It is also a low-cost manufacturing process.

A high-temperature module design may have a profound impact on power electronics and energy conversion technologies. For commercial applications, the new packaging and bonding process technology can be used in its current form, or can be scaled down to medium or conventional temperature ranges with a significantly reduced cost, making it a viable and economical option for large commercial markets such as hybrid electric vehicles, renewable energy conversion, and power supplies.

This work was done by John C. Elmes of Advanced Power Electronics Corporation, and Brian Grummel, Zehng John Shen, and Wendell Brokaw of the University of Central Florida for Glenn Research Center. Further information is contained in a TSP (see page 1).

Inquiries concerning rights for the commercial use of this invention should be addressed to NASA Glenn Research Center, Innovative Partnerships Office, Attn: Steven Fedor, Mail Stop 4–8, 21000 Brookpark Road, Cleveland, Ohio 44135. Refer to LEW-19091-1/2-1.

Quad First Stage Processor: A Four-Channel Digitizer and Digital Beam-Forming Processor

NASA's Jet Propulsion Laboratory, Pasadena, California

A 4-channel digitizer was designed, built, and tested. The very large, complex board enables SweepSAR. The proposed Deformation, Eco-Systems, and Dynamics of Ice Radar (DESDynl-R) L-band SAR instrument employs multiple digital channels to optimize resolution while keeping a large swath on a single pass. High-speed digitization with very fine synchronization and digital beam forming are necessary in order to facilitate this new technique.

The Quad First Stage Processor (qFSP) was developed to achieve both the processing performance as well as the digitizing fidelity in order to accomplish this sweeping SAR technique. The qFSP utilizes high-precision and high-speed analog-to-digital converters (ADCs), each with a finely adjustable clock distribution network to digitize the channels at the fidelity necessary to allow for digital beam forming. The Xilinx-produced FX130T Virtex 5 part handles the processing to digitally calibrate each channel as well as filter and beam-form the receive signals.

Demonstrating the digital processing required for digital beam forming and digital calibration is instrumental to the viability of the proposed DESDynl instrument. The qFSP development brings this implementation to Technology Readiness Level (TRL) 6.

This work was done by Chung-Lun Chuang, Scott J. Shaffer, Robert F. Smythe, Eric N. Liao, Samuel S. Li, Arin C. Morfopoulos, Louise A. Veilleux, Chester N. Lim, and Noppasin Niamsuwan of Caltech for NASA's Jet Propulsion Laboratory. Further information is contained in a TSP (see page 1). NPO-48936

Protective Sleeve for a Pyrotechnic Reefing Line Cutter

The sleeve provides improved operation of a parachute reefing system.

Lyndon B. Johnson Space Center, Houston, Texas

A metallic sleeve provides protection and guidance for the actuating lanyard pull of a parachute system reefing line cutter. This device ensures that the reefing line cutter is not damaged during packing or deployment. In addition, the device ensures that the actuating lanyard that initiates the cutter is pulled within the device's specification cone angle. Combined, these features increase the durability of the reefing line cutter used in parachute reefing systems, and significantly increases the reliability of the underlying reefing cutter. Protecting such a critical element of the controlled deployment of parachutes significantly improves the operation of the parachute reefing system.

The sleeve is designed as an "add on" component to provide lanyard pull guidance and cutter bending resistance. The end user can procure off-the-shelf hardware with no changes, and then choose to add the cutter sleeve at a later time based on usage and environment. This metallic sleeve is reusable and allows for a decrease in unit cost of the reefing line cutter.

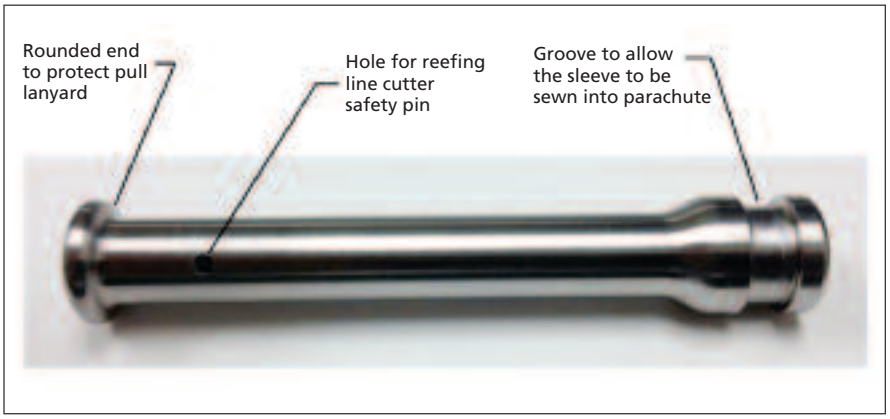

The **Cutter Sleeve** features a round end to protect the pull lanyard, a hole for the reefing line cutter safety pin, and a groove that allows the sleeve to be sewn into the parachute.

The cutter sleeve provides containment of gases or shrapnel in the event of an unexpected cutter failure/rupture. It also provides a more positive retention location, in the form of a groove around its diameter, for attachment to a parachute through stitching/sewing. Testing of reefing line cutters without the protective sleeve resulted in failures that included broken pull loops and bent cutters. Testing with the protective sleeve resulted in all cutters functioning correctly.

This work was done by James H. McMichael, Hai D. Nguyen, Mark Landeck, and Richard Hagen of Johnson Space Center. Further information is contained in a TSP (see page 1). MSC-25523-1

Metabolic Heat Regenerated Temperature Swing Adsorption

Liquid CO_2 as a coolant will not contaminate the area as it is sublimated from the life support system for heat rejection.

Lyndon B. Johnson Space Center, Houston, Texas

Two fundamental problems facing the development of a portable system to sustain life on extraterrestrial surfaces are (1) heat rejection and (2) rejection of metabolically produced CO_2 to an environment with a $ppCO_2$ of 0.4 to 0.9 kPa as is present on Mars. Portable life support systems typically use water for heat rejection via sublimation. Consequently, the water is removed from the life support system and into the surrounding environment after use. This wastes a valuable resource required for human life that is expensive to transport from Earth. Furthermore, rejecting the water vapor to the surrounding environment contaminates it, severely interfering with any search for life on extraterrestrial surfaces. A portable life support system should be able to use a variety of fluids for heat rejection, especially liquid CO_2, as it can be easily acquired and cheaply stored on the surface of Mars. The use of liquid CO_2 as a coolant has the advantage that it will not interfere with scientific investigations by contaminating the area as it is sublimated from the life support system for heat rejection.

A subsystem has been developed for a portable life support system (PLSS) called Metabolic heat regenerated Temperature Swing Adsorption (MTSA). MTSA simultaneously addresses heat rejection and CO_2 rejection to an environment ranging from vacuum to a $ppCO_2$ of 0.9 kPa or greater. The invention utilizes an adsorbent-based subsystem that is cooled with liquid CO_2, and is used to cleanse the vent loop of metabolically produced CO_2. Once the adsorbent is fully loaded with metabolically produced CO_2, metabolic waste heat from the expired breath is used to warm and regenerate the adsorbent bed. Exhausted adsorbent cooling fluid is used to aid in additional heat rejection and further cool the user.

The basic principle is removal of CO_2 by an adsorbent with regeneration

through temperature swing adsorption (TSA) over the temperature range bound by the sublimation temperature of CO_2 (less than 195 K) and the metabolic vent loop (310 K). There are two beds to facilitate continuous removal of metabolically produced CO_2 from the vent loop: one for loading the adsorbent via a vent loop exiting the helmet/undergarment of an astronaut's portable life support system, and another for regenerating the adsorbent.

This work was done by Taber MacCallum of Paragon Space Development Corp. for Johnson Space Center. Further information is contained in a TSP (see page 1). MSC-24859-1

CubeSat Deployable Log Periodic Dipole Array

Any small satellite with a need for a VHF antenna might benefit from this design, in addition to communications and military applications.

NASA's Jet Propulsion Laboratory, Pasadena, California

The antenna is composed of two main deployable structural components that help it achieve the large packing factor necessary to fit within the small volume of the CubeSat. The primary component of the antenna array is a tension stiffened truss, which is preloaded using a large tape spring. The truss bays are formed from solid discs connected by thin Kevlar thread. The Kevlar threads are set up in a hexapod configuration, and are fully tensioned and preloaded from the force of the tape spring, which runs through the center of the truss. The truss gets its overall stiffness from the properties and configuration of these Kevlar wires.

There are 21 elements on the antenna corresponding to the full desired frequency range of 30 to 300 MHz. The assembly, including cable spooler and motor, fits within a 2-U CubeSat. This is achieved by keeping the dipole discs thin, and by stacking them back-to-back. Additionally, the tape spring boom rolls up on itself to provide excellent stowed volume.

When stowed, the dipoles are sandwiched inside the fixed tube of the CubeSat, and cannot deploy until they are forced outward by the tape spring. To ensure the hexapod thread does not get tangled or frayed during antenna stowing and deployment, a scheme was devised where each individual wire is wrapped in a figure-eight configuration around two posts. The wire is laid on top of itself in subsequent wraps around the posts, with little chance of forming a tangle or knot. When the discs are pulled apart, there is minimal force required to dislodge the wire from the posts. This thread management scheme is effective; however, it does have drawbacks in that it is very tedious and requires several sets of hands working simultaneously. The posts also serve a dual purpose and provide a torsional locking feature between adjacent discs.

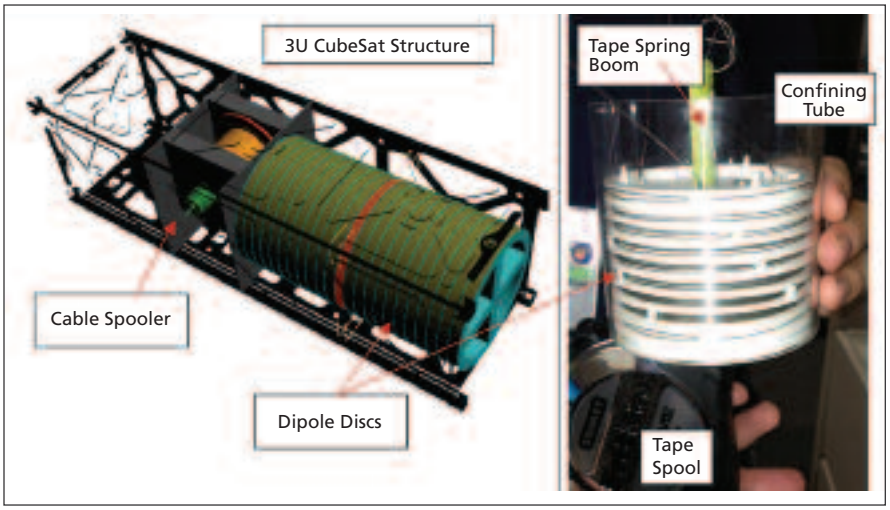

The **Antenna Array** assembly, including cable spooler and motor, fits within a 2-U CubeSat. At left is a CAD model of the VHF array stowed in a 3U CubeSat structure; at right is the initial stowed prototype of the LPDA.

This work was done by Mark W. Thomson, Vine M. Bach, Phillip E. Walkemeyer, Daniel L. Kahn, Andrew Romero-Wolf, and Samuel C. Bradford of Caltech for NASA's Jet Propulsion Laboratory. Further information is contained in a TSP (see page 1). NPO-49107

Re-entry Vehicle Shape for Enhanced Performance

A convex structure is used with a continuous slope.

Ames Research Center, Moffett Field, California

A vehicle entering the atmosphere of a planet will do so at hypersonic speeds and will need to decelerate and maneuver through that atmosphere while protecting its payload from excessive heating. As a consequence, the vehicle shape must be designed to provide optimal aerodynamic lift and drag properties, while minimizing convective and radiative heating to the vehicle outer surfaces.

These needs are met by this invention, which provides a convex structure with a continuous slope that can be described by four linear segments and six curvilinear segments joined together to provide a convex shape defined by nine parameters. Viewed parallel to the y-axis in a Cartesian coordinate system,

the projected cross-sectional shape includes first and second linear segments, spaced apart from each other and located on opposite sides of an *x*-axis, with each of the first and second segments being oriented substantially at a selected non-zero angle θ_c relative to the *x*-axis, each segment having a first segment end of closest approach to the *x*-axis with each closest approach segment end being located at substantially the same distance *R* from the *x*-axis. The projected shape includes a third linear segment that is oriented substantially perpendicular to the *x*-axis adjacent to the end of closest approach to the *x*-axis for each of the first and second linear segments.

The present invention provides an improvement over prior blunt body shapes in that the shape is actually of a class of geometric shapes that is describable by a relatively small number of geometry-shape parameters, and that provides a broad range of geometric shapes with favorable aerodynamic and aerothermal properties. These properties can then be analyzed by optimization methods for desired performance.

Optimization of the vehicle geometry-shape parameters can, for example, minimize heating levels subject to constraints that reduce aerodynamic performance, such as lift/drag, or can minimize weight of a thermal protection system, allowing a greater payload. Other properties can be optimized or established as constraints on a geometric parameter search, such as a requirement that a minimum lift/drag be met or exceeded, while minimizing center of gravity offset from vehicle centerline, to ease packing of a working vehicle while in space operations.

This work was done by James L. Brown, Joseph A. Garcia, and Dinesh K. Prabhu of Ames Research Center. Further information is contained in a TSP (see page 1).

Inquiries concerning rights for the commercial use of this invention should be addressed to the Ames Technology Partnerships Division at 1-855-NASA-BIZ (1-855-6272-249) or sumedha.garud@nasa.gov. Refer to ARC-15606-1.

NanoRacks-Scale MEMS Gas Chromatograph System

This is a compact, simple, cost-effective system.

NASA's Jet Propulsion Laboratory, Pasadena, California

In order to study atmospheric or evolved gases, it is highly advantageous for an instrument (e.g. mass spectrometer (MS), thermal conductivity detector (TCD)) to simplify the gas stream with a front-end gas chromatograph (GC). When used for planetary missions, high-performance GCs have to satisfy the additional challenging requirements of surviving high inertial loads with low mass, power, and volume in order to be included in Ventures-, Discovery- and New Frontiers-class missions in today's budget-constrained reality.

The development and adoption of advanced MEMS-GCs at JPL would provide a key enabling technology for near-term missions to Mars or Venus. A MEMS (Micro-Electro-Mechanical Systems)-based GC system would be significantly smaller, about 1 kg (including electronics), with a power consumption of less than 1 W (for isothermal operation). It would also not have the many complicated fittings and joints of a conventional GC, significantly enhancing inertness and robustness.

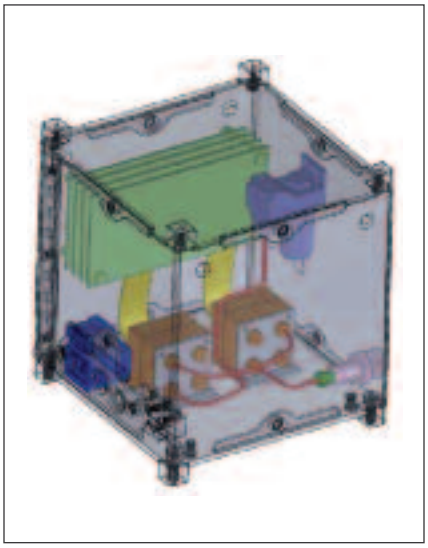

MEMS-GC System Model includes the MEMS-GC chip (with MEMS-preconcentrator (PC), MEMS-valves, MEMS-column in the middle of a Vespel block), a MEMS-thermal conductivity detector (TCD, in a separate Vespel block), a miniature diaphragm sample pump, and electronics. Mass: 1 kg, power: 1 W (peak 5 W), size: 4×4×4 in. (≈10×10×10 cm) (A 1U NanoLabs module).

JPL partnered with Cbana Labs to couple their MEMS-GC to a miniaturized adaptation of a JPL ion trap mass spectrometer, a version of which is currently operating in the Vehicle Cabin Atmosphere Monitor (VCAM) on the International Space Station (ISS). However, since a MEMS-GC has never flown in space before, JPL is looking at ways to reduce risk and to test the MEMS-GC cheaply and rapidly using the NanoRacks service to the ISS.

The MEMS-GC system includes the MEMS-GC chip (with MEMS-preconcentrator, MEMS-valves, MEMS-column in the middle of a Vespel block), a MEMS-TCD (in a separate Vespel block), a miniature diaphragm sample pump, and electronics. Cabin air would be used as the carrier gas.

This work was done by Richard D. Kidd, Murray R. Darrach, Vachik Garkanian, and Stojan Madzunkov of Caltech; and Byunghoon Bae of Cbana Labs for NASA's Jet Propulsion Laboratory. Further information is contained in a TSP (see page 1). ***NPO-48859***

Variable Camber Aerodynamic Control Surfaces and Active Wing Shaping Control

Concepts are examined to reduce aerodynamic drag and decrease fuel consumption.

Ames Research Center, Moffett Field, California

A new concept of aircraft aerodynamic control surfaces has been developed in connection with another new concept of active wing shaping control for reducing aircraft drag that will result in less fuel burn. The first concept is referred to as a variable camber continuous trailing edge flap or, alternatively, a variable camber continuous leading edge slat. The variable camber trailing edge flap (or leading edge slat) comprises multiple chord-wise segments (three or more) to form a cambered flap surface, and multiple span-wise segments to form a continuous trailing edge (or leading edge) curve with no gaps that could be prescribed by a mathematical function or the equivalent with boundary conditions enforced at the end points to minimize tip vorticities. Aerodynamic simulations have shown that this type of flap can reduce aerodynamic drag substantially as compared to a conventional flap. A new active wing-shaping control concept is proposed in connection with the presently disclosed variable camber continuous trailing edge flap (or leading edge slat). The active wing-shaping control is designed to change a wing shape in-flight in order to achieve a desired optimal wing shape for optimal drag reduction.

Currently, as fuel is burned, wing loading is reduced and causes the wing shape to change in bending and twist. This wing shape change causes the wings to be less aerodynamically efficient. This problem can be further exacerbated by modern high aspect flexible wing design. Aircraft designers typically address the fuel efficiency goal by usually reducing aircraft weights, improving propulsion efficiency, and/or improving the aerodynamics of aircraft wings passively. In so doing, the potential drag penalty due to changes in the wing shapes would still exist at off-design conditions.

The unique or novel features of the new concepts are:

1. Variable camber flap provides the same lift capability for lower drag as

compared to a conventional flap.

2. Continuous trailing edge flap (or leading edge slat) provides a continuously curved trailing edge (or leading edge) with no gaps to minimize vorticities that can lead to an increase in drag.
3. The active wing-shaping control method utilizes the novel flap (or slat) concept described herein to change a wing shape to improve aerodynamic efficiency by optimizing span-wise aerodynamics.
4. An aeroelastic method for analyzing wing deflection shape under aerodynamic loading is used in a wing-control algorithm to compute a desired command for the flap-actuation system to drive the present flap (or slat) system to the correct position for wing shaping.

This work was done by Nhan Nguyen of Ames Research Center. Further information is contained in a TSP (see page 1).

Inquiries concerning rights for the commercial use of this invention should be addressed to the Ames Technology Partnerships Division at 1-855-NASA-BIZ (1-855-6272-249) or sumedha.garud@nasa.gov. Refer to ARC-16644-1.

Spacecraft Line-of-Sight Stabilization Using LWIR Earth Signature

Applications could include remote science and planetary science missions, Earth surveillance and reconnaissance, and deep space optical communication.

NASA's Jet Propulsion Laboratory, Pasadena, California

Until the time of this reporting, when a space vehicle required a reference signal for inertial pointing, the choices were a signal beacon from an Earth location, the Earth radiance in the visible spectrum, or a star tracker. However, limitations can arise from using these techniques. For example, the signal beacon suffers from limited signal power (either in RF or optical) and will constrain the application to limited ranges, errors due to stray-light and centroiding limit the accuracy of a star tracker, and the spatial/temporal variability of the Earth's albedo and its illumination by the Sun introduces limitations when used in the visible or near infrared light.

To bypass these limitations, the bright and near-uniform image of the Earth in the LWIR (long wavelength infrared) (8 to 13 micron) may be used to obtain a reference signal for inertial stabilization and pointing of a spacecraft platform.

The potential of using the bright and near-uniform Earth thermal infrared (or LWIR) signature as a stable reference for accurate (microrad or less) inertial pointing and tracking of an optical communication beacon onboard a space vehicle was investigated, including the determination of the fundamental limits of applicability of the proposed method for space missions in deep space. In the thermal infrared, Earth's emission appears relatively uniform and is independent of the Sun's illumination. Therefore, it can be used as a stable pointing reference.

Objective of the stabilization is to align the Earth's image along the de-

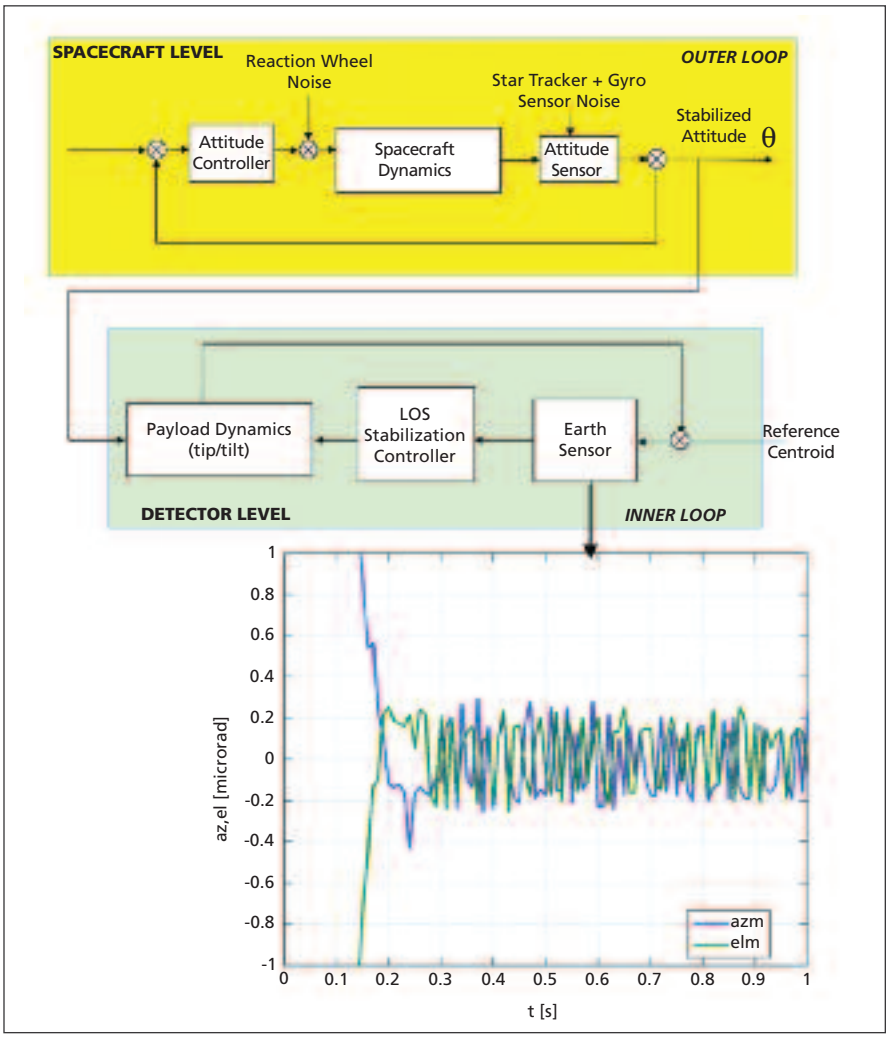

The brightness and near-uniformity of the **Earth LWIR Signature** as a function of range indicates its great potential as a stable reference for inertial pointing of planetary spacecraft, when the Earth is not fully illuminated by the Sun. This figure shows the multistage stabilization block diagram, and the resulting time history of the detector line-of-sight azimuth and elevation angles with respect to a reference datum onboard the spacecraft, and demonstrates that submicroradian stabilization accuracy is achievable with a multistage line-of-sight stabilization approach.

sired line of sight (LOS) in the face of existing system disturbances. Because of the submicroradian precision levels required by high-precision pointing, a large dynamic range is involved in the dynamic response of the pointing system. Hence, the pointing and tracking algorithms are based on a multistage approach that includes: (a) a coarse stage (outer loop) based on sequential loop closure of a vehicle attitude stabilization feedback control loop at a low control bandwidth (10^{-3} to 10^{-1} Hz) to compensate for typical attitude control disturbances; followed by (b) a fine stage (inner loop) based on an image boresight stabilization feedback loop at higher frequencies that makes use of an articulated (tip/tilt) fast steering mirror to track the Earth's LWIR reference signal in the image plane.

A simulation package has been developed that generates spacecraft and gimbaled camera dynamic model, inputs realistic spacecraft disturbances, stabilizes the spacecraft attitude dynamics via a proportional-integral-derivative (PID) control loop at 0.01 Hz, propagates the azimuth and elevation states of the dynamics of the detector plane, adds the sensor noise model to the computed detector azimuth and elevation based on a detector model and centroiding algorithm, and stabilizes the detector line-of-sight via PID control at 100 Hz. A block diagram is shown in the figure.

A comparison of the performance of a quantum-well infrared photodetector sensor array using data from actual space-qualified components has been carried out. Preliminary results involving the effect of the sensor performance on the LOS system stabilization have been studied. Using realistic noise spectra from the Mars Reconnaissance Orbiter mission, simulations demonstrated that submicroradian stabilization accuracy, shown in the figure as time history of the detector line-of-sight azimuth and elevation angles with respect to a reference datum on-board-the spacecraft, is feasible using this approach.

This work was done by Marco B. Quadrelli and Sabino Piazzolla of Caltech for NASA's Jet Propulsion Laboratory. For more information, contact iaoffice@jpl.nasa.gov. NPO-48934

Technique for Finding Retro-Reflectors in Flash LIDAR Imagery

Lyndon B. Johnson Space Center, Houston, Texas

Orbital rendezvous and docking of two spacecraft is a topic of continued interest to NASA. For crewed missions, it is frequently the case that the target is cooperative (i.e., is equipped with some sort of navigation aid). If one of the relative navigation instruments is a Flash LIDAR, then this aid may be a suite of retro-reflectors. One of the most difficult aspects of this problem (especially at close range) is finding the retro-reflectors in a Flash LIDAR image amongst a substantial amount of clutter.

A new technique has been developed for autonomously finding the three-dimensional location of candidate retro-reflectors in a Flash LIDAR image. With no a-priori state information, this new approach is capable of finding an analyst-defined number of reflectors. It is effective at rejecting most bright non-reflector objects. This technique, which continues to be developed and tested, has substantially better performance (finds more reflectors, with fewer false positives) than simpler approaches with only a modest increase in computational resources.

The Orion/Multi-Purpose Crew Vehicle is a new crewed vehicle being designed by NASA and Lockheed Martin for piloted exploration missions capable of destinations beyond low Earth orbit (LEO). The vehicle will also maintain the capability to perform rendezvous, proximity operations, and docking (RPOD) with other orbital assets and elements in the exploration architecture. The vision navigation sensor (VNS) is a Flash LIDAR, and will be the primary navigation instrument used by the Orion during the RPOD flight phase. Thus, maturing techniques for finding reflectors in Flash LIDAR imagery of cooperative vehicles is critical to the current Orion relative navigation architecture.

This work was done by John A. Christian of Johnson Space Center. Further information is contained in a TSP (see page 1). MSC-25237-1

Novel Hemispherical Dynamic Camera for EVAs

John H. Glenn Research Center, Cleveland, Ohio

A novel optical design for imaging systems is able to achieve an ultra-wide field of view (UW-FOV) of up to 208°. The design uses an integrated optical design (IOD). The UW-FOV optics design reduces the wasted pixels by 49% when compared against the baseline fisheye lens. The IOD approach results in a design with superior optical performance and minimal distortion.

This work was done by Jason Geng of Xigen LLC for Glenn Research Center. Further information is contained in a TSP (see page 1).

Inquiries concerning rights for the commercial use of this invention should be addressed to NASA Glenn Research Center, Innovative Partnerships Office, Attn: Steven Fedor, Mail Stop 4–8, 21000 Brookpark Road, Cleveland, Ohio 44135. Refer to LEW-18984-1.

Software

360° Visual Detection and Object Tracking on an Autonomous Surface Vehicle

This software addresses the problem of an autonomous vehicle patrolling a region for objects of interest using multiple cameras. The system must identify and track the objects over time and localize their positions in the world. It implements an autonomous perception and situation awareness system, which receives images from an omnidirectional camera head, identifies objects of interest in these images, and probabilistically tracks the objects' presences over time, even as they may exist outside of sensor range.

The software consists of three functional parts. The Image Server records the images from all cameras on the camera head simultaneously. It also records the data from the inertial navigation system (INS) that provides the vehicle pose at the image frame. Next, the Image Server stabilizes the images to produce images with horizontal, image-centered horizons. Finally, in addition to passing on the images and pose to the next system for further processing, the Image Server efficiently logs this large amount of data for offline use.

The Contact Server detects objects of interest in the stabilized images and calculates the absolute bearing of each contact. Two object-detection algorithms are employed, loosely trained on templates of the 3D objects of interest. Additionally, the Contact Server adjusts the images for better detection results; for example, adjusting for variable lighting conditions.

The Object-level Tracking and Change Detection (OTCD) Server integrates the information from the Contact Sever over time and over all cameras to probabilistically track the objects of interest and to detect changes of interest. OTCD maintains a database of hypothesized true objects, along with a probability of existence that measures the confidence that the object exists at its hypothesized location at a given time. Finally, OTCD can send downstream alerts when a new object appears or a known object disappears.

The software detects objects of interest from arbitrary perspectives and widely varied lighting conditions, and localizes and tracks these objects over time. It tracks the existence of these objects in their estimated positions, even when they are out of sensor range, enabling a patrol vehicle to leave and come back and hypothesize whether the same objects of interest are in the same position viewed earlier (change detection). The software integrates information for multiple source cameras to provide a 360° view of the environment, and tracks objects seamlessly as they transition between cameras. It includes several helpful analysis utilities, such as a real-time remote viewer of the scene and identified objects, efficient multi-leveled data logging, and the capability to process data logs offline for replays.

This work was done by Michael Wolf, Yoshiaki Kuwata, Christopher Assad, Robert D. Steele, Terrance L. Huntsberger, David Q. Zhu, Andrew Howard, and Lucas Scharenbroich of Caltech for NASA's Jet Propulsion Laboratory. For more information, contact iaoffice@jpl.nasa.gov.

This software is available for commercial licensing. Please contact Dan Broderick at Daniel.F.Broderick@jpl.nasa.gov. Refer to NPO-47850.

Simulation of Charge Carrier Mobility in Conducting Polymers

Electric conduction in polymers is one of the key elements in avoiding catastrophic internal electrostatic discharge in dielectrics during space missions. This software package enables the simulation of carrier mobility for any given site concentration, which is a material design parameter that can be varied in experimental studies. The software computes the charge mobility for a disordered network of carrier sites. The mobility is obtained by computing the average drift velocity for an applied electric field. The mobility is given by the ratio of the drift velocity to the electric field.

The software uses an efficient Monte Carlo technique to sample the transit time of carriers injected on one end of the simulation domain. The mobility can be obtained as a function of temperature and site concentration, which are parameters of interest for experiments and materials design.

This software is implemented in C++ and is highly modular. New models and variations in the simulation process can easily be added. Parallelization for execution on a distributed computing platform was implemented.

This program enables the calculation of charge mobility in polymers with varying dopant concentration, as a function of electric field and temperature. The objective is to use this program to explore the parameter space and identify the material parameters that best meet the design requirements. The program will be used to optimize a new material system and will help solve the problem of catastrophic internal electrostatic discharges in dielectrics, which is one of the largest sources of anomaly or failure in space missions. Deep space missions to the outer planets and their moons, where the radiation environment is particularly harsh, will benefit most from the new modeling capability.

This work was done by Paul A. Von Allmen and Seungwon Lee of Caltech for NASA's Jet Propulsion Laboratory. For more information, contact iaoffice@jpl.nasa.gov.

This software is available for commercial licensing. Please contact Dan Broderick at Daniel.F.Broderick@jpl.nasa.gov. Refer to NPO-48727.

Observational Data Formatter Using CMOR for CMIP5

The current software has been developed to work on NASA instrument datasets, an upgrade over similar software that only worked on datasets from climate model output. NASA is attempting to reformat satellite data to fit the specific and highly detailed data format and metadata requirements for CMIP5 (Coupled Model Intercomparison Project Phase 5). This software has relieved science data teams from multiple instruments from the task of understanding and conforming to the CMIP5 data requirements.

The software reads in netcdf files, combined with select metadata input from the user, and intelligently calls functions from the CMOR (Climate Model Output Rewriter) library to write out new netcdf files in the proper format for inclusion in CMIP5. Currently, the software is capable of ingesting data from AIRS (Atmospheric Infrared Sounder), MLS (Microwave Limb Sounder), TES

(Tropospheric Emission Spectrometer), MODIS (Moderate Resolution Imaging Spectroradiometer), AVISO (French space agency data provider), and QuikSCAT (Quick Scatterometer).

The unique feature is integration of the CMOR function library, written in C, with code able to understand the output of science data teams. Many conventions used in the climate modeling community differ radically from those used in the observational data community, and this software serves as a bridge between the two.

This work was done by Steven J. Lewis of Caltech for NASA's Jet Propulsion Laboratory. For more information, contact iaoffice@jpl.nasa.gov.

This software is available for commercial licensing. Please contact Dan Broderick at Daniel.F.Broderick@jpl.nasa.gov. Refer to NPO-48258.

Propellant Loading Physics Model for Fault Detection Isolation and Recovery

Microsoft Excel spreadsheet is used to simulate the operation.

John F. Kennedy Space Center, Florida

A Fault Detection, Isolation and Recovery (FDIR) system needs some internal concept of how the monitored system operates. This "operating concept" needs mathematical logic to represent the cause and effect relationship between constituent components of the system, health and status of those components, and the resulting health and status of the overall system. Models constructed with commercial simulation systems such as MATLAB and Simulink may ignore individual component contribution to system operation. Instead, the modeler may naturally focus on overall system parameters with lumped values representing the individual component characteristics. The resulting simulations faithfully calculate overall system operation, but may miss anomalies that occur because of plugged, stuck, or otherwise inoperable individual components.

This innovation is a spreadsheet written for Microsoft Excel with equations that simulate cryogenic propellant loading system operating characteristics. The spreadsheet takes commands from an operator to open and close valves, change pump speeds, and change pressure set-points. The spreadsheet continuously calculates the operating state of the propellant loading system including measurements such as pressures, flow rates, pump speeds, and tank levels. The simulation is component-oriented, containing comprehensive mathematical descriptions of valves of different types and sizes, pneumatic supply system pumps, filters, and tanks. An "antagonist" operator may introduce faults in certain of the components. The spreadsheet simulates the effects of the introduced faults.

The software simulates operation of the Simulated Rapid Propellant Loading (SRPL) System hardware at the KSC Cryogenics Laboratory. The Excel spreadsheet uses Active Control buttons and sliders drawn in Excel that allow valves to be opened and closed and pumps to be controlled at various speeds. Other Active Control sliders allow the antagonist operator to introduce faults in all the components that make up the physics model of the SRPL.

The Excel spreadsheet has a unique update feature that calculates the pressures, temperatures, and flows in the physics model of the SRPL. The update feature calculates all these values, then waits one second and recalculates based on updated tank levels, ullage quantities, and bulk liquid temperatures. Thus, the spreadsheet is capable of continuously updating the liquid levels integrating flow rates and heat flux in the system in real time.

Equations can be translated into C code and used in the embedded processor. The results calculated by the C code can be validated easily by comparing calculated values to the output of the spreadsheet.

This work was done by Charles Goodrich, Rebecca Oostdyk, Mark Lewis, and Christopher Forney of Kennedy Space Center. Further information is contained in a TSP (see page 1). *KSC-13631*

Probabilistic Guidance for Swarms of Autonomous Agents

A probabilistic approach is simpler to implement as the number of agents becomes large.

NASA's Jet Propulsion Laboratory, Pasadena, California

Available guidance approaches for large numbers (i.e., swarms) of artificial agents are currently very limited. Swarms in nature (e.g., bees, birds, ants) typically contain hundreds to thousands of agents. The problem is how to mimic nature, and develop guidance laws for artificial (man-made) swarms containing hundreds to thousands of artificial agents.

A new guidance solution lets go of conventional deterministic approaches and instead looks at statistical approaches. Because swarms contain a statistically meaningful number of agents, a probabilistic approach is more relevant to the problem. In particular, a probabilistic guidance approach (PGA) has been developed that controls the statistical ensemble (i.e., the desired probability density across a swarm of agents), rather than any single individual agent's trajectory. Because the PGA works with a statistically large ensemble of agents, the "law of large numbers" kicks in, and the PGA approach actually becomes more accurate and simpler to implement as the number of agents becomes large. This is in sharp contrast to deterministic approaches to swarm guidance that become more complex and unwieldy as the number of agents becomes large.

The main idea is to have each agent follow an independent realization of a Markov chain. The desired distribution emerges as the ensemble of agents in the swarm maneuvers about, asymptotically achieving a desired statistical steady-state condition, and eliciting a clear emergent behavior from the swarm. The implementation of the probabilistic guidance law is completely decentralized, and leads to an important swarm behavior that exhibits au-

tonomous self-repair and maintenance capabilities.

The development area relies heavily on the theory of Markov processes, Monte-Carlo-Markov-Chain sampling methods, graph theory, and Lyapunov stability analysis. The development is aided by recent research in designing fast mixing Markov chains that converge to desired distributions and incorporate constraints on transition probabilities, and many classical results on convergence of Markov chains.

The main novel feature is that the PGA guidance law is probabilistic in nature, and specifies the desired spatial probability density distribution for the swarm rather than the exact desired paths of the individual agents. Consequently, PGA is a more natural and useful guidance statement when dealing with swarms comprised of a statistically large number of agents, compared to deterministic methods that become unwieldy as the number of agents becomes large.

This work was done by David S. Bayard and Behcet Acikmese of Caltech for NASA's Jet Propulsion Laboratory. For more information, contact iaoffice@jpl.nasa.gov.

The software used in this innovation is available for commercial licensing. Please contact Dan Broderick at Daniel.F.Broderick@jpl.nasa.gov. Refer to NPO-47851.

Reducing Drift in Stereo Visual Odometry

The drift was reduced from an uncorrected 47 cm to just 7 cm.

NASA's Jet Propulsion Laboratory, Pasadena, California

Visual odometry (VO) refers to the estimation of vehicle motion using onboard cameras. A common mode of operation utilizes stereovision to triangulate a set of image features, track these over time, and infer vehicle motion by computing the apparent point cloud motion with respect to the cameras. It has been observed that stereo VO is subject to drift over time.

It is well known that stereo triangulation suffers from bias induced from correlation error (i.e., subpixel errors in matching between features in the left and right images of a stereo pair). The nature of this bias is a complicated function of the error statistics of the correlation and depends on scene structure, camera configuration, and imaging geometry. The goal of this work was to better characterize the stereo bias than has been done to date, and explore the effect of compensating for this bias on VO drift.

The problem was approached in terms of a stochastic propagation of error from the image plane to triangulation. The end result is a better representation of stereo bias than has been accomplished thus far. In early tests, this stereo bias correction has had a dramatic effect in reducing VO drift. In a simulated run of 100 m, the drift was reduced from an uncorrected 47 cm to just 7 cm. The preliminary conclusion is that VO drift is due primarily to stereo bias rather than to inherent bias in the non-linear estimator used to recover motion.

Given a model of noise in correlation matching between the left and right images of a stereo pair, the projection of any point in the world into the stereo pair can be indexed by its pixel location in the left image and the horizontal shift of that location in the right image, referred to as disparity. Thus, every point in the world that is simultaneously visible in both cameras can by described as (x,y,d). Considering only integer values, a lookup table was constructed and indexed by (x,y,d), where (x,y) spans the whole of the left image, and d spans values corresponding to reasonable ranges in the scene. At each (x,y,d), the assumed noise profile is taken from correlation and a Monte Carlo simulation is performed to propagate that noise profile into the triangulated point in space. The results are stored in a table indexed by image column, row, and disparity.

Given any point correspondence, the corresponding (x,y,d) is looked up, interpolated from integer to real values as required, and the triangulation statistics are extracted. The lookup table generation is a one-time process for any calibrated imaging system, and the subsequent lookup has minimal computational overhead. From the triangulation statistics, the likely bias is taken and added directly to the triangulated point. In ensemble, this produces a point cloud with higher fidelity than the uncorrected cloud and, consequently, a better incremental VO estimate.

VO bias compensation has focused primarily on correcting the motion estimate rather than on correcting the stereo. This method can be implemented in real-time on a deployed system and shows very promising preliminary results.

This work was done by Adnan I. Ansar of Caltech for NASA's Jet Propulsion Laboratory. For more information, contact iaoffice@jpl.nasa.gov.

This software is available for commercial licensing. Please contact Dan Broderick at Daniel.F.Broderick@jpl.nasa.gov. Refer to

Future Air-Traffic Management Concepts Evaluation Tool

An aircraft monitoring system and an aircraft user system can interact and negotiate changes with each other.

Ames Research Center, Moffett Field, California

In the United States, as many as 7,000 commercial and private aircraft may be in the air simultaneously at any given time and date, and the total number of commercial flights in a given 24-hour period generally exceeds 50,000. To maintain the safety and efficiency of air travel, this innovation receives proposed flight plans and associated flight route information and flight parameters for aircraft operating in a given region (e.g., the continental United

States), and provides actual flight routes and schedules based on expected air traffic. This innovation avoids or minimizes air traffic incidents by changing one or more flight plan parameters where appropriate, for one or more of these aircraft.

This innovation comprises methods for evaluating and implementing air traffic management tools, and approaches for managing and avoiding an air traffic incident before an incident can occur. A first system receives parameters for flight plan configurations (e. g., initial fuel carried, flight route, flight route segments followed, flight altitude for a given flight route segment, aircraft velocity for each flight route segment, flight route ascent rate, flight route descent rate, flight departure site, flight departure time, flight arrival time, flight destination site and/or alternate flight destination site), flight plan schedules, expected weather along each flight route segment, aircraft specifics, airspace (altitude) bounds for each flight route segment, and what navigational aids are available.

The invention provides flight-plan routing and direct routing, or wind optimal routing, using great-circle navigation and spherical Earth geometry. It also provides for aircraft dynamic effects, such as wind effects at each altitude, altitude changes, airspeed changes, and aircraft turns to provide predictions of aircraft trajectory and, optionally, aircraft fuel use.

A second system provides several aviation applications using the first system. Several classes of potential incidents are analyzed, and averted, by appropriate changes en route of one or more parameters in the flight plan configuration, as provided by a conflict detection and resolution module and/or traffic flow management modules. These applications include conflict detection and resolution, miles-in-trail or minutes-in-trail aircraft separation, flight arrival management, flight re-routing, weather prediction and analysis, and interpolation of weather variables based upon sparse measurements.

This work was done by Banavar Sridhar, Kapil S. Sheth, Gano Broto Chatterji, Karl D. Bilimoria, Shon Grabbe, and John F. Schipper of Ames Research Center. Further information is contained in a TSP (see page 1).

Inquiries concerning rights for the commercial use of this invention should be addressed to the Ames Technology Partnerships Division at 1-855-NASA-BIZ (1-855-6272-249) or sumedha.garud@nasa.gov. Refer to ARC-14653-2.

Examination and *A Priori* Analysis of a Direct Numerical Simulation Database for High-Pressure Turbulent Flows

Minkowski functionals are employed that provide the geometrical, topological, and morphological aspects of isosurfaces.

NASA's Jet Propulsion Laboratory, Pasadena, California

A previously created direct numerical simulation (DNS) database of mixing of species under supercritical pressure has been examined and analyzed for the purpose of understanding the modeling requirements in the context of large eddy simulation (LES). Of particular interest is reproducing in LES the feature of uphill species diffusion that is identified in DNS. The examination of the database was performed by employing Minkowski functionals that provide the geometrical, topological, and morphological aspects of isosurfaces that are extracted from a field through computing dimensionless shapefinders: genus, planarity, and filamentarity.

The analysis is restricted to simply connected isosurfaces having a null genus. Isosurfaces of the second invariant of the deformation tensor and of the dissipation calculated as a result of all transport processes were found to be quite different; those derived from the second invariant turned out to have more randomness when compared to those derived from the dissipation that had better defined volumetric extent. Upon filtering, at the same filter width, there were more structures of greater extent and with well-defined morphology resulting more from the dissipation than from the second invariant.

Independent of the filter width, the dissipation-related isosurfaces had more complex structure than those issued from the second invariant, as evidenced by larger planarity and filamentarity. In general, the structures originating from the second invariant were filamentary, a feature that was retained when filtering, whereas those originating from the dissipation had more comparable planarity and filamentary values. Having thus examined the template LES solution, the activity of terms in the differential LES equations was examined and, in addition to the classical subgrid-scale (SGS) terms issued from the convective terms of the original equations, other SGS terms were identified.

When evaluated on the database, some of these new terms were shown to have important contributions in the LES equations. The importance of the contribution of each term increased with increasing pressure. Several models were proposed and tested for these significant SGS terms with the goal of preserving, in future LES, the features observed in the template LES solution. The model that best reduced the error on all terms compared to the template values was based on an Approximate Deconvolution Model combined with explicit filtering that succeeded in reducing the error by more than a factor of two on terms occurring in the momentum, species, and energy equations. Particularly crucial was the effect of the model for recovering the flux of species experiencing uphill diffusion, a phenomenon identified for multi-species but not for binary-species mixing. Based on this study, caution is advised on simply extrapolating results from supercritical-pressure binary-species mixing to multi-species mixing.

This work was done by Josette Bellan and Giulio Borghesi of Caltech for NASA's Jet Propulsion Laboratory. For more information, contact iaoffice@jpl.nasa.gov. NPO-49179

Resource-Constrained Application of Support Vector Machines to Imagery

Fast computation of the SVM decision function over an image using minimal RAM.

NASA's Jet Propulsion Laboratory, Pasadena, California

Machine learning techniques have shown considerable promise for automating common visual inspection tasks. For example, Support Vector Machine (SVM) classifiers that have been learned from labeled training data deliver strong detection performance both for finding human faces in photographs and locating geologic landforms such as craters and volcanoes in planetary images gathered by spacecraft. However, SVMs are computationally expensive to apply to an image using the traditional spatial scanning method in which a rectangular window is slid across the image one pixel at a time and the SVM is evaluated on each patch of pixels under the window. The new software uses small fast Fourier transforms (FFTs) and the overlap-and-add technique from signal processing to quickly and efficiently compute the exact SVM decision function over an entire image using minimal random access memory (RAM).

SVMs classify a feature vector by computing a weighted combination of kernel evaluations between the feature vector and a set of "support vectors." The support vectors are positive and negative examples from the training set that were identified during the learning phase. Each kernel evaluation is essentially a nonlinear measurement of the similarity between the feature vector and a given support vector. For many of the commonly used kernels, the kernel evaluation can be expressed as a linear dot product between the feature vector and the support vector followed by additional nonlinear operations. The linear part of the computation actually dominates the workload, which enables the software to achieve a significant speedup by performing the linear calculations over the entire image with FFTs. A further refinement uses the overlap-and-add technique to limit the amount of RAM required. Overlap-and-add computes small, localized FFTs and then pieces partial results together to establish the final answer.

The software provides an effective way to apply SVMs to image data and is particularly well suited for resource-constrained environments such as onboard a spacecraft. The technique allows exact computation of the SVM decision function over an image using minimal RAM (typically less than 5% of the size of the image). Also, the approach is complementary to "reduced set" methods, which speed up SVM calculations by reducing the number of support vectors required. Used together, the two methods can yield a multiplicative gain in performance. The software implementation is not specific to any particular domain. Thus far, it has been demonstrated for the crater detection problem; however, in principle, it can be used for a variety of image inspection tasks. One could envision a variety of smartphone apps based around the ability to take a picture and detect/classify/count objects in the picture.

This work was done by Michael C. Burl of Caltech, and Philipp G. Wetzler of the University of Colorado, Boulder for NASA's Jet Propulsion Laboratory. Further information is contained in a TSP (see page 1).

The software used in this innovation is available for commercial licensing. Please contact Dan Broderick at Daniel.F.Broderick@jpl.nasa.gov. Refer to NPO-48072.


NASA
National Aeronautics and
Space Administration